JOURNAL OF SOLID STATE CHEMISTRY 110, 58–65 (1994)

Chemical Bonding in Stoichiometric and Substoichiometric Vanadium Nitride

Ľ. Benco

Institute of Inorganic Chemistry, Slovak Academy of Sciences, Dúbravská cesta 9, 842 36 Bratislava, Slovakia

Received December 3, 1992; in revised form April 27, 1993; accepted August 6, 1993

A band structure calculation is performed for VN and $VN_{0.75}$ assuming long-range ordered vacancies at the nonmetal lattice sites in the latter system. Chemical bonding is discussed in terms of total, partial, and differential density of states. Crystal orbitals are visualized by means of molecular orbital cluster calculation. *Strong σ and π chemical bonds are enabled across the vacancy* by removing N atoms. The metal–metal bond is strengthened and the metal–nitrogen bond is weakened in the vacant system. The extreme hardness and unusual thermal behavior are in good agreement with the picture of the conjugated system of π bonds interconnected in three dimensions. © 1994 Academic Press, Inc.

INTRODUCTION

The rocksalt type structure substoichiometric nitrides of the group IV and V transition metals show important physical properties (1). They have been attracting considerable technical (2–4) and theoretical (5–10) interest. The electronic structures of these systems are similar. Two peaks, which can be attributed to the "vacancy" states, always appear some eV under the Fermi level. The vacancy-induced creation of new bonding states (compared to the stoichiometric compound) agrees well with the thermodynamical stability of the substoichiometric materials. New octahedral bonds are formed between the metal atoms surrounding the vacancy. Many studies using a large variety of methods have been devoted to the electronic structure calculation of vacant systems, but the role of vacancy and its stabilizing effect in bonding conditions, induced by the vacancy, has not been understood yet. The goal of this work is to gain insight into the chemical bonding of the system with vacancy as compared to the stoichiometric one.

The representative example of the above-mentioned compounds is cubic VN_x. Its sodium chloride type structure consists of two sublattices with the nitrogen atoms located in the octahedral interstitial positions of the vanadium host lattice. The stable compounds cover the broad composition range $0.66 \leq x \leq 0.996$ (2) with vacancies only on the N sublattice. Within this composition range VN_x significantly changes its physical, thermodynamic, and mechanical properties (1). One of the most remarkable changes is decreasing hardness with increasing nitrogen content, i.e., the higher the concentration of the vacancies in the vanadium nitride, the higher the hardness of the vanadium nitride.

We study the chemical bonding of VN_x on the base of supercell band structure calculation and molecular orbital cluster calculation, respectively. The vacancy-ordered $VN_{0.75}$ has the same superstructure as $TiC_{0.75}$ and $TiN_{0.75}$ (8). It represents the system with a high content of ordered vacancies. The long-range ordered structures were found in the composition range $VN_{0.74}$–$VN_{0.84}$ (11), so that the supercell approach is fully justified.

COMPUTATIONAL DETAILS

The tight binding scheme based upon the extended Hückel method (12) is used to obtain the electronic structure of the stoichiometric and vacant vanadium nitride, respectively. The atomic parameters used for our calculations are summarized in Table 1.

Although the symmetry of both structures is $Fm3m$ (14), the symmetry of the unit cells differs. For the purpose of simple comparison we choose so-called "computational"

TABLE 1
Atomic Parameters for Extended Hückel Calculations[a]

Atom	*Orbital*	H_{ii}	$\zeta_{i1}(c_1)$	$\zeta_{i2}(c_2)$
N	2*s*	−26.0	1.95	
	2*p*	−13.4	1.95	
V	4*s*	−8.81	1.30	
	4*p*	−5.52	1.30	
	3*d*	−11.0	4.75 (0.4755)	1.70 (0.7052)

[a] H_{ii}, orbital ionization energies (eV); ζ_{ij}, Slater exponents; c_j, coefficients in the double-zeta expansion of the *d* orbitals.

0022-4596/94 $6.00

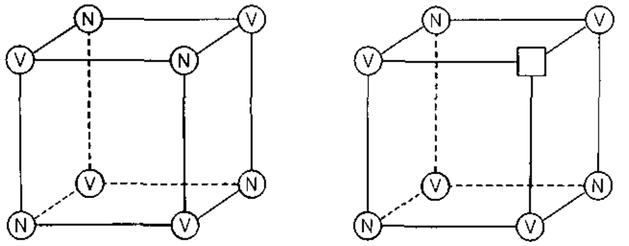

FIG. 1. The computational unit cells for stoichiometric VN (left) and ordered vacant model structure $VN_{0.75}$ (right).

unit cells. The structure of the stoichiometric crystal VN and/or ordered substoichiometric crystal $VN_{0.75}$ is generated by translation of computational unit cells shown in Fig. 1 along translation vectors (the same vectors as for simple cubic unit cell). For stoichiometric VN this computational unit cell is four times larger than the basic unit cell (two atoms in the face-centered basic unit cell). Nevertheless, the choice of the larger computational unit cell enables us not only to compare them with band structures of both systems but to compare them with band structures of titanium nitrides TiN and $TiN_{0.75}$ (8) as well. The model ordered structure $VN_{0.75}$ consists of transition metal atoms with coordination number six ($V^{[6]}$) and four ($V^{[4]}$). The vacancy $\square_N$ is octahedrally surrounded by six $V^{[4]}$ atoms which have only four nearest N neighbors. The $V^{[6]}$ atoms are surrounded by six N neighbors as in stoichiometric VN.

RESULTS AND DISCUSSION

(*a*) *Band Structure*

Band structures of VN and $VN_{0.75}$ are shown in Fig. 2. In the case of stoichiometric VN, the use of the larger unit cell, whose symmetry differs from the that of the face-centered basic unit cell, results in the backfolding of the bands. The backfolding is outlined in Fig. 3. Here the form of the lowest energy levels along the path $\Gamma \rightarrow X$ of the simple cubic unit cell is schematically shown as a result of the folding of the lowest energy levels along the path $\Gamma \rightarrow X \rightarrow W$ of the face-centered cubic unit cell. Although the band structure is thus more complicated, it is directly comparable to that in Fig. 2b.

Let us look at the band structure of stoichiometric VN first. The nitrogen *s* levels are situated in the energy interval -30 to -26 eV. These levels are not interesting from the chemical bonding point of view and are not shown in Fig. 2.

The nitrogen *p* levels are in stoichiometric VN spread over a narrow energy interval ~ -16.0 to ~ -12.7 eV. The *p* levels are separated from the metal *d* levels except for the nearest neighborhood of the Γ point. The small bandwidth and the little overlap with the *d* band indicate little bonding interaction of the nitrogen *p* orbitals with the orbitals of the neighboring atoms.

The *d* band ranges from -13.0 to 3.7 eV. It consists of two components. The octahedral coordination of metal atoms split *d* orbitals into t_{2g} symmetry orbitals (d_{xy}, d_{xz},

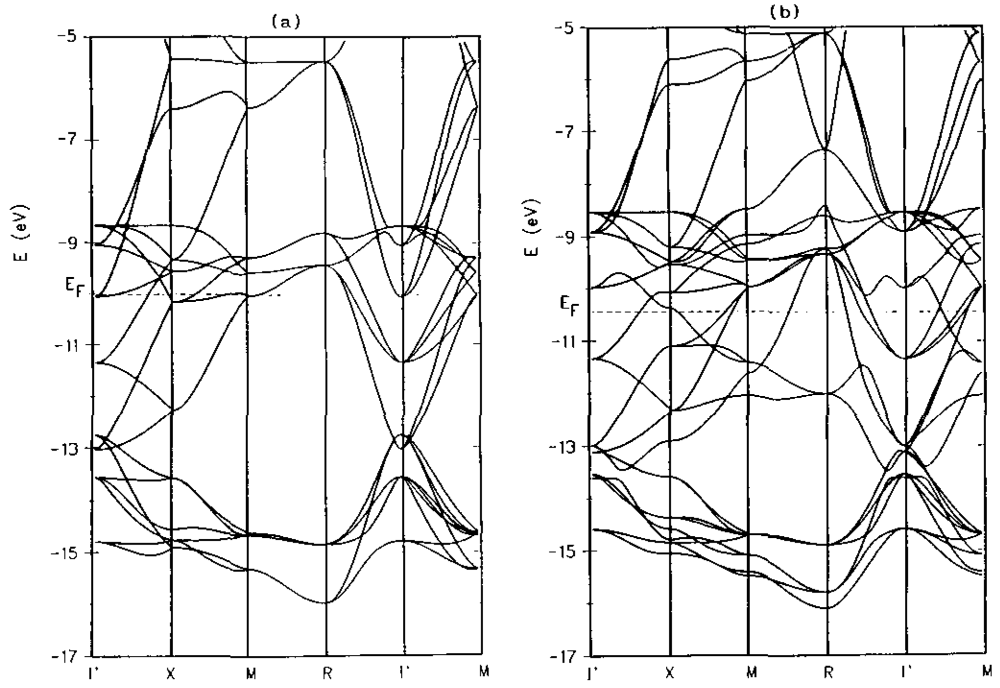

FIG. 2. The band structure of VN (a) and ordered $VN_{0.75}$ (b).

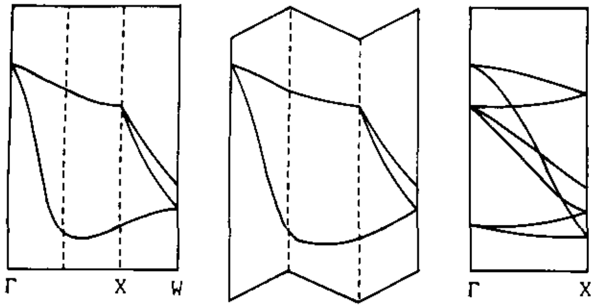

FIG. 3. The schematic diagram showing the backfolding of the three lowest p levels of the fcc unit cell along the $\Gamma \rightarrow X \rightarrow W$ path into the lowest p levels along the $\Gamma \rightarrow X$ path of the simple cubic unit cell.

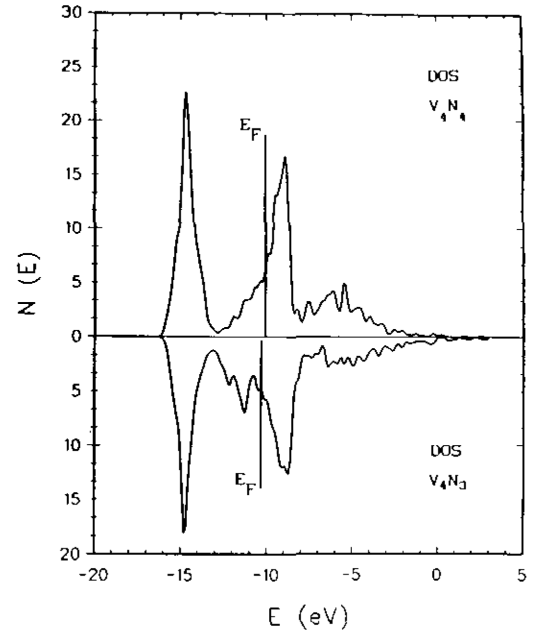

FIG. 4. The total DOS for VN and ordered $VN_{0.75}$ per computational unit cell. The Fermi levels are also indicated.

d_{yz}) and e_g symmetry orbitals ($d_{z^2}, d_{x^2-y^2}$). The t_{2g} level band ranging from -13.0 to -8.7 eV overlaps with the e_g level band (-10.1 to 3.7 eV). The band structure along the path connecting the high symmetry points of the Brillouine zone shows that the e_g level band is situated above the Fermi level ($E_F = -10.018$ eV), except for the nearest neighborhood of the Γ point. Although in the stoichiometric VN the e_g orbitals point toward the neighboring nitrogen atoms, the character of their interaction is predominantly antibonding. As the energy levels of the metal s and p crystal orbitals are situated too high above the Fermi level to be involved into bonding interactions, these are not shown in Fig. 2.

The band structure of the ordered vacant system $VN_{0.75}$ is similar to that of stoichiometric VN. The s orbital levels remain in the energy interval -30.0 to -26.0 eV. The shape of the p band is very little changed. The number of the p levels is lowered from 12 for eight-atom unit cell V_4N_4 to nine for seven-atom unit cell V_4N_3. The very pronounced change is a shift of some d levels toward the lowered energy. These so called "vacancy states" are seen in Fig. 2b in the region of point R at -12.0 eV as a triply degenerated level. The shift of the levels into the bonding region causes the Fermi level to be lowered to the value $E_F = -10.429$ eV.

(*b*) *Density of States*

Figure 4 displays the total density of states (DOS) of VN and ordered $VN_{0.75}$. The main components of DOS are shown in Figs. 5 and 6 for VN and $VN_{0.75}$, respectively. In both systems the first intensive narrow band at about -15 eV consists of the nitrogen p orbitals with a small amount of metal d orbitals. The metal s and p orbitals contribute very little to this band. The d band is spread from about -14.5 to ~0 eV. In the stoichiometric VN the d band consists of two components t_{2g} and e_g. The t_{2g} part of the band is situated at lower bonding energies. The Fermi level divides the t_{2g} component of the d band into bonding and nonbonding states. The t_{2g} partial density of states

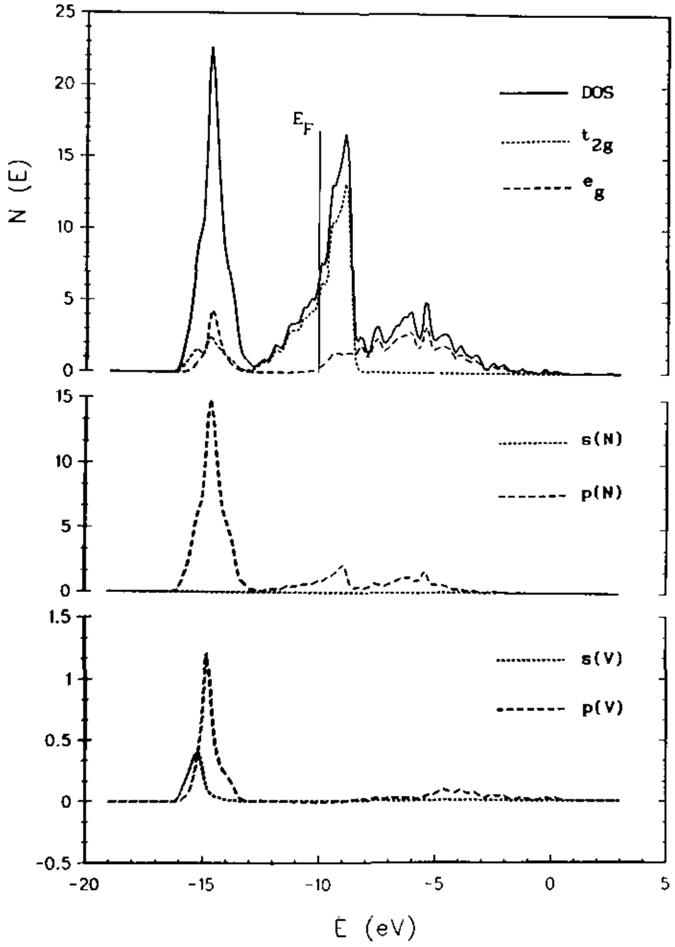

FIG. 5. The main components of the total DOS for VN.

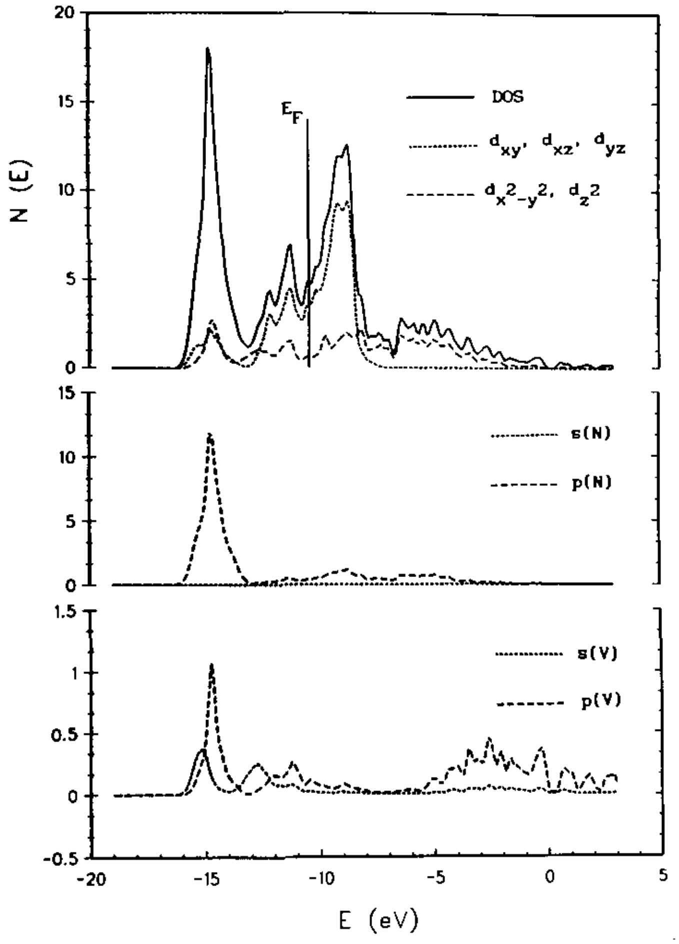

FIG. 6. The main components of the total DOS for $VN_{0.75}$.

increases toward the Fermi level. About 1 eV above it the density of nonbonding states reaches the maximum. The e_g component of the d band is situated above the Fermi level except for the very small part coming from the vicinity of the Γ point, as already shown in Fig. 2a. Two new features are worth noting in the DOS of the ordered vacant system. First, the two-maxima band of "vacancy states" appears in the lower part of the d band; second, the shape of the d band is changed. The band maximum is lowered and broadened. The intensity of the upper part of the band above −8 eV is lowered too. In Fig. 6, where individual components of the band are displayed, we see that the change of the d band shape is caused by partial density of states coming from the $d_{x^2-y^2}$ and d_{z^2} orbitals. These components of DOS are not limited to the nonbonding and antibonding energy region, and they are spread throughout the whole d band. In other words, the $d_{x^2-y^2}$ and d_{z^2} orbitals which are nonbonding in the stoichiometric VN become the components of chemical bonds. Figure 7 displays the $V^{[4]}$ and $V^{[6]}$ components of the total DOS. We see that the vacancy states come from four coordinated metal atoms. The $V^{[6]}$ contribution to the total density of states is shaped in the same way as all the d components of DOS in the stoichiometric VN.

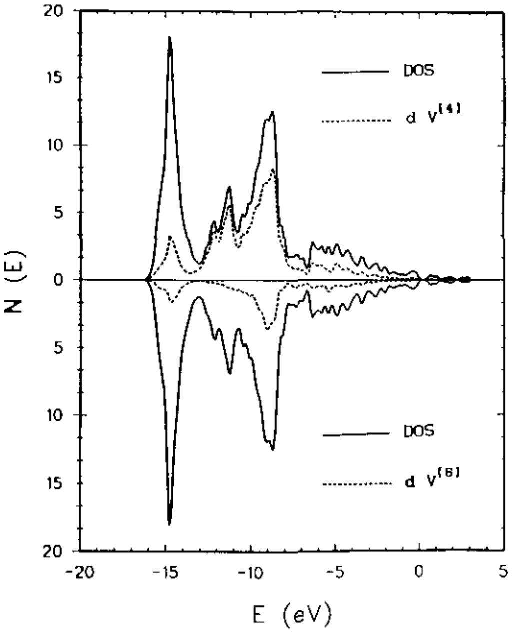

FIG. 7. The comparison of the partial $V^{[4]}$ d DOS and the $V^{[6]}$ d DOS.

The DOS changes induced by the vacancy are presented in Fig. 8 in terms of the total density of states differential curve (ΔDOS). This curve is calculated according to

$$\Delta DOS = DOS(V_4N_3) - DOS(V_4N_4). \qquad [1]$$

Both expressions on the right-hand side of Eq. [1] are normalized to one couple of atoms, VN. Two main components $\Delta d(V)$ and $\Delta p(N)$ are also presented in Fig. 8.

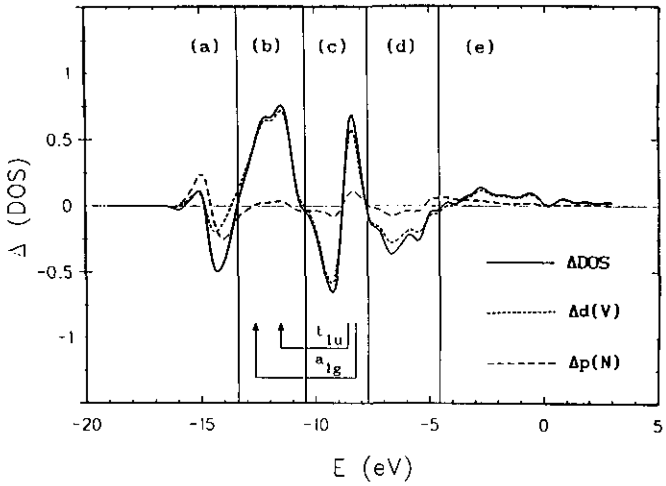

FIG. 8. The total DOS differential curve and two main components $\Delta d(V)$ and $\Delta p(N)$. Two arrows indicate the shift of two levels induced by removing the central nitrogen atom from the cluster $V_{14}N_{12}N$.

The component curve $\Delta d(V)$ illustrates the fact that the electronic structure changes due to the altered metal *d* orbital bonding. The *p* orbitals play a very small role in this process, and the role of all other orbitals (i.e., the nitrogen *s* orbitals and the vanadium *s* and *p* orbitals) could be neglected. The band area above the zero line represents the new states appearing in the process of vacancy creation ($V_4N_4 \rightarrow V_4N_3\square$). The band area equals the number of new states normalized to one couple of atoms, VN. The bands below the zero line are the states which vanish in the process of vacancy creation. The vertical lines divide the ΔDOS curve in Fig. 8 into five regions (a)–(e). Region (a) corresponds to the intense *p* orbital nitrogen band. Although one can hardly distinguish changes in these bands in Fig. 4, these changes are well pronounced in the ΔDOS curve in Fig. 8. The contribution of *d* orbitals to this band is lowered and the whole nitrogen *p* orbital band is shifted toward the lower binding energies. Region (b) represents the vacancy states. The large density of states increase is due solely to the metal *d* orbitals. As we can see from Fig. 7 all $V^{[4]}$ *d* orbitals are contributing to this band. The densities of the nonbonding state changes near the *d* band maximum above the Fermi level are expressed in region (c). Both the nitrogen *p* and metal *d* states are shifted to higher energies, the latter being more prevalent. The large density of states decreasing occurs in region (d). This energy region covers stoichiometric VN nonbonding crystal orbitals consisting mainly of the metal *d* orbitals of e_g symmetry ($d_{x^2-y^2}$, d_{z^2}). Both the band structure (see Fig. 2) and partial DOS of the two systems (see Figs. 5 and 6) show that in $VN_{0.75}$ these two *d* orbitals become the components of the crystal orbitals with energy levels below the Fermi level. This means the increasing DOS in region (b) is attributed to the DOS decrease in energy region (d). In energy region (e) the density of state does not show any substantial changes.

(*c*) *A Comparison of the Solid with the Cluster*

Our solid-state results are made clearer by a comparison with the results of the molecular orbital cluster calculation. The unit cells (the clusters) taken into the cluster calculation differ from the solid-state computational unit cells shown in Fig. 1. We choose clusters having the same central atom point symmetry as the solid-state nitrogen atom has (see Fig. 9). After the removing of the nitrogen atom from the center of the cluster its point symmetry remains the same. This enables us to assign the energy levels of one cluster to the other one and evaluate the electronic structure changes induced by removing the central nitrogen atom. The assignment is shown in Fig. 10. Nitrogen *s* orbital levels are again not included in the molecular orbital (MO) scheme. The group of the MO levels scattered across the energy interval −15 to −14 eV consists mainly of nitrogen *p* orbitals. The second large group of MO levels at the energy interval −12 to −8 eV are vanadium *d* orbital levels. The levels at energies higher than −8 eV contain a large contribution of the unoccupied vanadium *s* and *p* orbitals. The electronic structure changes occurring after removing the central nitrogen atom are as follows.

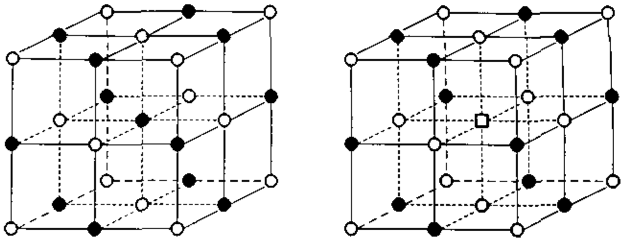

FIG. 9. The clusters of atoms $V_{14}N_{12}$ surrounding the central nitrogen atom (left) and the vacancy (right). (●) N atoms, (○) V atoms, and (□) the vacancy.

Two levels suffer large shift. Both these levels contain a large contribution from the central nitrogen atom orbitals in the initial cluster $V_{14}N_{12}N$. The first one is the triples t_{1u} level, and the second nondegenerate one has the symmetry a_{1g}. Both levels are not occupied in cluster $V_{14}N_{12}N$, and become occupied in vacant cluster $V_{14}N_{12}\square$.

The levels which contain a small amount of the central nitrogen orbitals in initial cluster $V_{14}N_{12}N$ are shifted very little. The direction of their moving depends on the new position of two energy levels a_{1g} and t_{1u}. The other levels of the same symmetry are repelled from them. The stabilizing shift of the three *p* levels toward the lower binding

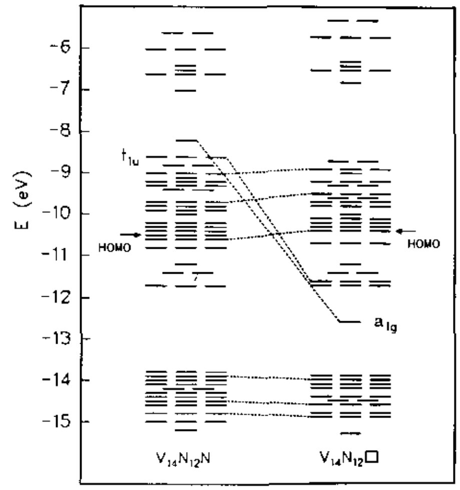

FIG. 10. The molecular orbital scheme of two clusters $V_{14}N_{12}N$ and $V_{14}N_{12}\square$, respectively. The mutual assignment is shown only for shifted levels. The highest occupied molecular orbitals (HOMO) are indicated by arrows. The number of the horizontal lines represents the degeneracy degree of the level.

energies is outlined in Fig. 10. On the other hand, the three *d* levels are shifted toward the higher energies. The lowest one even becomes unoccupied in the cluster $V_{14}N_{12}\square$.

The energy levels not containing contribution from central nitrogen orbitals are practically unaffected by the removal of the central nitrogen atom.

The two molecular orbitals a_{1g} and t_{1u}, which dramatically change on going from the cluster $V_{14}N_{12}N$ to the cluster $V_{14}N_{12}\square$, are visualized in Figs. 11 and 12. The a_{1g} orbital is the typical σ antibonding orbital in the cluster $V_{14}N_{12}N$. It consists mainly of the *d* orbitals of vanadium atoms octahedrally surrounding the central nitrogen atom. The axial d_{z^2} orbitals and the equatorial $d_{x^2-y^2} + d_{z^2}$ orbitals pointing toward the center of the cluster are supposed to be able to create a strong σ bond. The central nitrogen atom contributes to this MO with the *s* orbital of the opposite sign of the charge density. This weakening of the charge density in the center of the cluster coming from the metal *d* orbitals prevents creating a strong σ bond, and the molecular orbital a_{1g} remains unoccupied with its energy level too high in the antibonding energy region. On the other hand, the obstructing *s* orbital is missing in the cluster $V_{14}N_{12}\square$. The *d* orbitals of six vanadium atoms which represent $V^{[4]}$ atoms octahedrally surrounding the vacancy in ordered $VN_{0.75}$ create a six-centered σ bond. The electron density maximum of the σ bond is in the center of the octahedra. The energy level belonging to this molecular orbital is even the lowest *d* energy level. This type of σ bond is described in substoichiometric $TiN_{0.75}$ (8), where bonding conditions are similar. The creation of the new bond is shown by means of electron density cuts. Herzig *et al.* (8), evaluating σ bonding interaction via the vacancy, have concluded that this can also occur between the two $Ti^{[4]}$ d_{z^2} orbitals oriented at right angles to each other. This conclusion is fair, but the interaction does not concern the d_{z^2} orbitals oriented at right angles to each other. Axial parts of the d_{z^2} orbitals of the apical metal atoms interact with the equatorial parts of the d_{z^2} orbitals of the other four metal atoms, all having the same orientation.

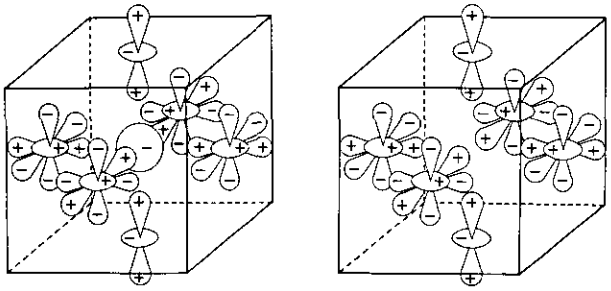

FIG. 11. The schematic indication of the main components of the a_{1g} molecular orbital. The central nitrogen *s* orbital prevents the creation of the multicentered σ bond (left). The bonding combination of the *d* functions after removing the central nitrogen atom (right).

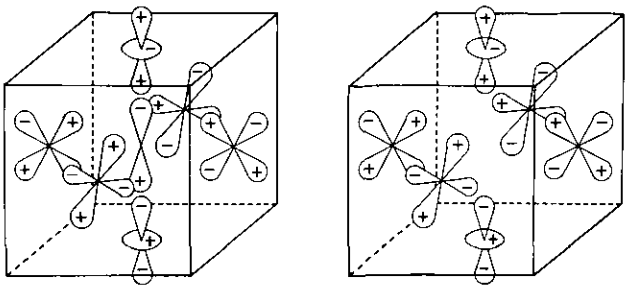

FIG. 12. Schematic indication of main components of one of the three parts of the t_{1u} molecular orbital. The central nitrogen p_z orbital prevents the creation of the multicentered π bond (left). The bonding combination of the *d* functions after removing the central nitrogen atom (right).

Contrary to the nondegenerate a_{1g} level representing the σ interaction of the *d* orbitals, the triply degenerate molecular orbital t_{1u} is created by the π interaction of the *d* orbitals of vanadium atoms octahedrally surrounding the center of the cluster. Only one of the three components of the t_{1u} MO, which contains d_{z^2} orbitals in apical positions, is shown in Fig. 12. The central nitrogen p_z orbital enters this MO again with opposite sign of the charge density thus obstructing the electron density increase and the formation of a strong π bond. After removing the central nitrogen atom the chemical bond becomes strong. Its energy level is shifted from −8.6 to −11.6 eV (see Fig. 10).

The energy level a_{1g} and t_{1u} shifts in the cluster induced by vacancy creating at central position are outlined in Fig. 8 by means of two arrows. The differential DOS curve displays the shift of bands possessing some bandwidth and band area representing the infinite number of energy levels. This fact should be borne in mind when we compare the shift of two cluster levels with the ΔDOS curve. The energy region −13 to −11 eV, in which new states appear in solid state, fits well with that into which the two levels are shifted in the cluster $V_{14}N_{12}\square$. The energy region (d) in which the decrease of the DOS occurs in the $VN_{0.75}$, as compared with the stoichiometric VN, does not fit with the energy region of the two t_{1u} and a_{1g} antibonding energy levels in the cluster $V_{14}N_{12}N$. The explanation is quite simple. The cluster point symmetry is the same as the symmetry of the Γ point. As we can see from the band structure of the stoichiometric VN (Fig. 2a), the energy levels of the whole *d* band are situated at energies some eV higher than the Γ point throughout the whole Brillouin zone. The energy region about 2 eV higher than the a_{1g} and t_{1u} energy levels on the left-hand side of Fig. 10 is equivalent to the region (d) from which the states are transferred to the region (b) in Fig. 8.

(*d*) *Overlap Populations*

The overlap population defined as $\Sigma c_i c_j S_{ij}$ is used to characterize the strength of chemical bonds (13). c_i and c_j are the coefficients of the linear combination of atomic orbitals. S_{ij} stands for the matrix element of the overlap between two atomic orbitals i and j. The overlap populations calculated for a couple of atoms in unit cells shown in Fig. 1 are given in Table 2. The rapid decrease of S_{ij} with distance causes low values of overlap populations except those for nearest neighboring atoms. This is illustrated with the values for atom pairs placed in the diagonal positions of cube faces. The strength of the bond between the metal atoms situated at a distance of the lattice parameter is demonstrated for a pair of atoms V–V′ with the vacancy placed in the middle, between them. Since the overlap population is changed with altered lattice parameter to be able to compare them, all values reported in Table 1 are obtained for the same geometry (the experimental geometry of the stoichiometric VN; a = 0.414 nm). Although bonds of the same kind can be compared for the two systems, we cannot directly compare the strength of the V–N and V–V bonds, respectively, because of the different bond length and geometry arrangement.

Let us discuss the N–N bonding first. Although the N–N distance is not large (r = 0.2927 nm), the interaction of two nitrogen atoms approaches zero. The geometry arrangement is the reason for this negligible interaction. The nitrogen atoms are placed in diagonal positions of cube faces. Their p orbitals are perpendicular to each other, and the overlap of the s orbitals is too small to create the effective chemical bond. The nitrogen atoms are thus bound in the structure solely via interaction with nearest-neighbor metal atoms.

The dominant components of the nitrogen–metal bonds are nitrogen p orbitals. Although only a small amount of the p and d orbitals is included in this bond (see Figs. 5 and 6), the p(N)–d(V) overlap is so high that the overlap population reaches large values for both systems compared. In vacant $VN_{0.75}$, two types of the metal atoms ($V^{[6]}$ and $V^{[4]}$) enter the V–N interaction. Note that the $V^{[4]}$–N bond strength is much weaker than the $V^{[6]}$–N one. The weakening of the $V^{[4]}$–N bond is caused by a decreasing amount of the $V^{[4]}$ d orbitals in these bonds. The reason for this decreasing is the formation of the metal–metal bonds via the vacancy into which the d orbitals in $VN_{0.75}$ are included to a much higher extent than into the metal–metal bonds via the nitrogen atom.

The geometry arrangement of the metal atoms is the same as that of the nitrogen atoms. The partially filled d orbitals enable the metal atoms to create weak metal–metal bonds across the nonmetal positions (see left-hand side of Figs. 11 and 12). The overlap population for $V^{[4]}$–$V^{[6]}$ differs very little from that for $V^{[6]}$–$V^{[6]}$. The increasing value for the pair $V^{[4]}$–$V^{[4]}$, as compared to the value for $V^{[6]}$–$V^{[6]}$, is in good agreement with the bond strengthening displayed in the right-hand side of Figs. 11 and 12.

The concept of a weak second-neighbor d_{z^2}–□–d_{z^2} bond via the vacancy, adopted in (8) for similar vacant systems $TiN_{0.75}$, would lead to the surprising conclusion that such interaction is very weak. The minus sign of the overlap population for the couple of atoms $V^{[4]}$–$V'^{[4]}$ indicates that this interaction is even antibonding. This result is not so surprising when we realize that the overlap of the d orbitals centered at metal atoms $V^{[4]}$ and $V'^{[4]}$ is very low. The chemical bond between atoms $V^{[4]}$ and $V'^{[4]}$ does exist (as shown in Figs. 11 and 12) in the form of σ and π bonds via the vacancy. The overlap of V and V′ d_{z^2} orbitals cannot be considered as the direct one. It is in both cases (σ and π bond, respectively) mediated by the d orbitals of all the other four $V^{[4]}$ atoms surrounding the vacancy. As the numerical procedure of the overlap population calculation works only with the direct overlap of the two atomic orbitals, this bond is not expressed through the increasing of the V–V′ bond, but indirectly through the increasing of the $V^{[4]}$–$V^{[4]}$ bond.

TABLE 2
Overlap Populations for the VN and $VN_{0.75}$

	Overlap population	
Couple of atoms	V_4N_4	V_4N_3
N–$V^{[6]}$	0.318	0.314
N–$V^{[4]}$	—	0.179
$V^{[6]}$–$V^{[6]}$	0.045	—
$V^{[4]}$–$V^{[4]}$	—	0.132
$V^{[4]}$–$V^{[6]}$	—	0.053
N–N	−0.003	−0.003
$V^{[4]}$–$V'^{[4]}$	−0.026	−0.029

CONCLUDING REMARKS

The electronic structures of the systems MN and $MN_{0.75}$ (M = Ti, V) are very similar. They differ only in some details, e.g., the shape of the vacancy band, its position under the Fermi level. The main common feature of the substoichiometric nitrides is the appearance of one nondegenerate σ and one triply degenerate π bond between the metal atoms across the vacancy. In the ordered systems $MN_{0.75}$, every other nitrogen position is vacant in all three dimensions. π bonds are thus interconnected into three-dimensional conjugated system of bonds schematically displayed in Fig. 13. In real systems, the vacancy ordering is not ideal but random. Every two neigh-

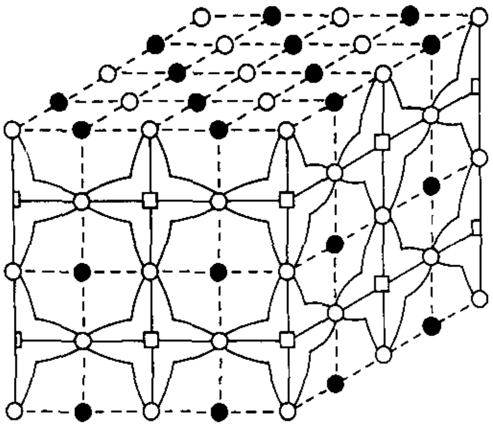

FIG. 13. The scheme of the interconnection of the multicentered σ and π bonds in three dimensions in the ordered $VN_{0.75}$. Solid lines stand for the metal–metal bonds, and dashed lines indicate the metal–nitrogen bonds. The symbols used are the same as in Fig. 9.

boring vacancies are interconnected by conjugated multicentered π bonds. Conjugated chains of bonds are randomly interrupted by nitrogen atoms, thus forming chains of various length interconnected in directions perpendicular to each other. These "whisker-like" interconnections lead not only to the thermodynamical stability of vacant systems over the broad composition range, but also to their fracture toughness.

The vacancy creation divides the metal atoms according to the coordination number into two groups ($V^{[6]}$ and $V^{[4]}$). The metal atoms with lowered coordination number create metal–metal bonds which are strengthened, and metal–nitrogen bonds which are weakened. In this work we deal only with two systems, VN and $VN_{0.75}$. The existence of stable compounds VN_x with x less than 0.75 means that the coordination number of some metal atoms is lowered to two, and such materials are even more interconnected by multicentered σ and π bonds than is outlined in Fig. 13. From this point of view, we can formulate the conclusion of this work more generally. The lower the coordination number of the metal atoms, the stronger metal–metal bonds become, and the weaker metal–nitrogen bonds become.

This generalization allows us to understand another interesting property of substoichiometric VN_x. Čapková *et al.* (14) have found that in the $VN_{0.74} \rightarrow VN_{0.89}$ series the thermal vibrations of metal atoms increase, and that for the sample $VN_{0.89}$ the thermal parameter of the metal reaches a value more than twice as large as that of the nitrogen atoms. On the other hand, the thermal parameter of the nitrogen atoms decreases with the increasing x. As we have already shown above (see Figs. 11 and 12) the nitrogen atom performs a double role in VN_x structures—bonding and antibonding. The strong covalent bond is formed by placing the nitrogen atom between the metal atoms. The degeneracy of the multicentered π bond is not removed but the character of the metal–metal bond becomes antibonding. With increasing the concentration of N atoms in their sublattice, the rigid skeleton of conjugated metal–metal bonds becomes more weakened. The bond becomes more plastic, and then thermal parameter of the metal atoms is increased. On the other hand the increase of vacancy concentration raises the strengthening of the metal sublattice, and weakening the metal–nitrogen bonds and larger thermal vibrations of nitrogen atoms is allowed.

REFERENCES

1. L. E. Toth, "Transition Metal Carbides and Nitrides." Academic Press, London, 1971.
2. W. Lengauer and P. Ettmayer, *J. Less-Common Met.* **109,** 351 (1985); W. Lengauer and P. Ettmayer, *Monatsh. Chem.* **117,** 713 (1986).
3. F. Kubel, H. D. Flack, and K. Yvon, *Phys. Rev. B* **36,** 1415 (1987); F. Kubel, W. Lengauer, and K. Yvon, *Phys. Rev. B* **38,** 12908 (1988).
4. S. Nagakura, T. Kusunoki, F. Kakimoto, and Y. Hirotsu, *J. Appl. Crystallogr.* **8,** 65 (1975); S. Nagakura and T. Kusunoki, *J. Appl. Crystallogr.* **10,** 52 (1977).
5. G. Ries and H. Winter, *J. Phys. F: Met. Phys.* **10,** 1 (1980).
6. A. Neckel, *Int. J. Quantum. Chem.* **23,** 1317 (1983).
7. P. Marksteiner, P. Weinberger, A. Neckel, R. Zeller, and P. H. Dederichs, *Phys. Rev. B* **33,** 812 (1986).
8. P. Herzig, J. Redinger, R. Eibler, and A. Neckel, *J. Solid State Chem.* **70,** 281 (1987).
9. P. Blaha and K. Schwarz, *Phys. Rev. B* **36,** 1420 (1987).
10. L. Skála and P. Čapková, *J. Phys.: Condens. Matter* **2,** 8293 (1990).
11. T. Onozuka, *J. Appl. Crystallogr.* **11,** 132 (1978).
12. M.-H. Whangbo, M. Evain, T. Hungbanks, M. Kertesz, S. D. Wijeyesekera, C. Wilker, C. Zheng, and R. Hoffmann, Quantum Chemistry Program Exchange No. 571 (1988).
13. S. D. Wijeyesekera and R. Hoffmann, *Organometallics* **3,** 949 (1984).
14. P. Čapková, Ĺ. Smrčok, V. Šíma, V. Valvoda, B. Chalupa, and P. Ettmayer, *Phys. Status Solidi B* **143,** 471 (1987).